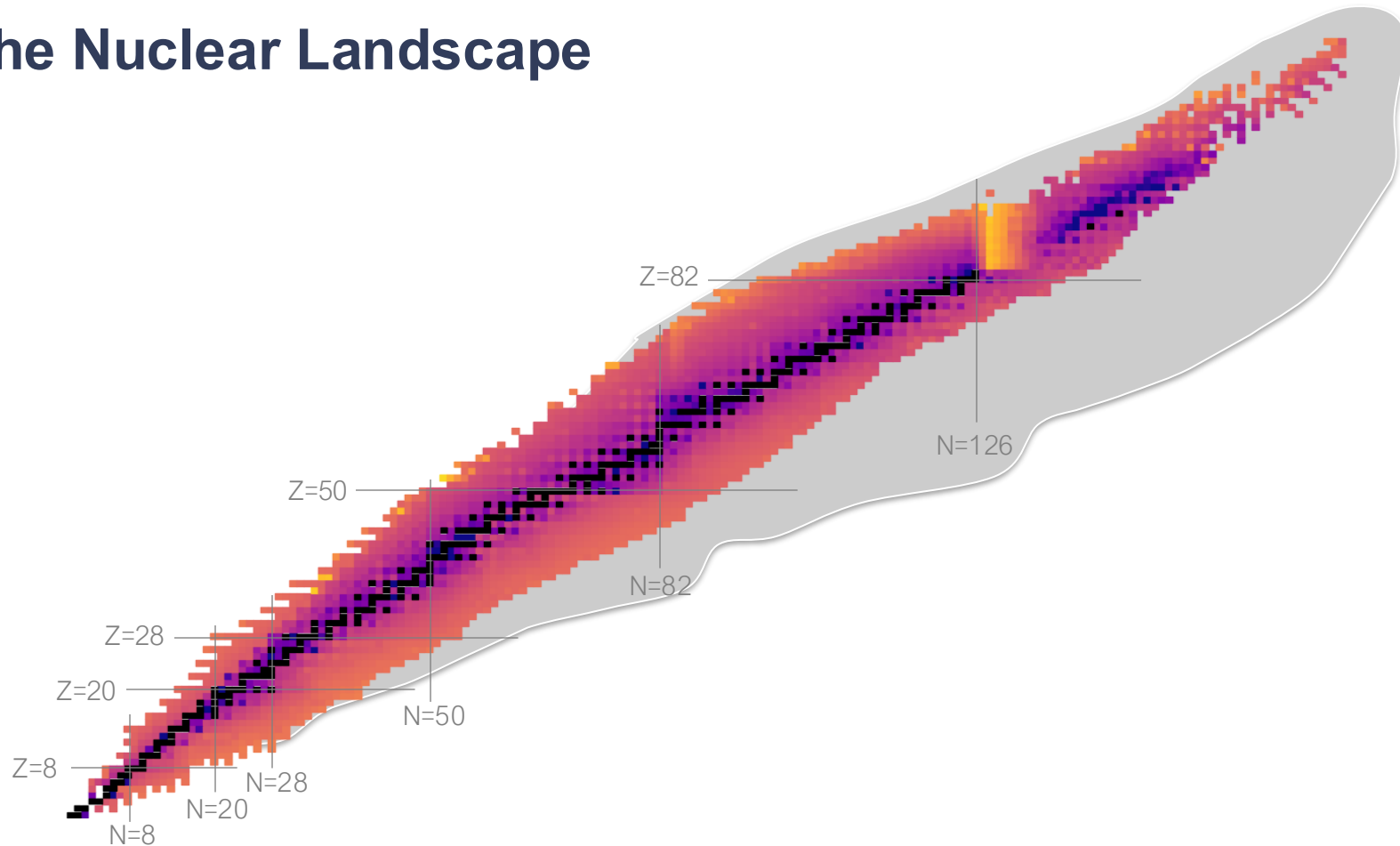


# Collectivity Across the Nuclear Chart

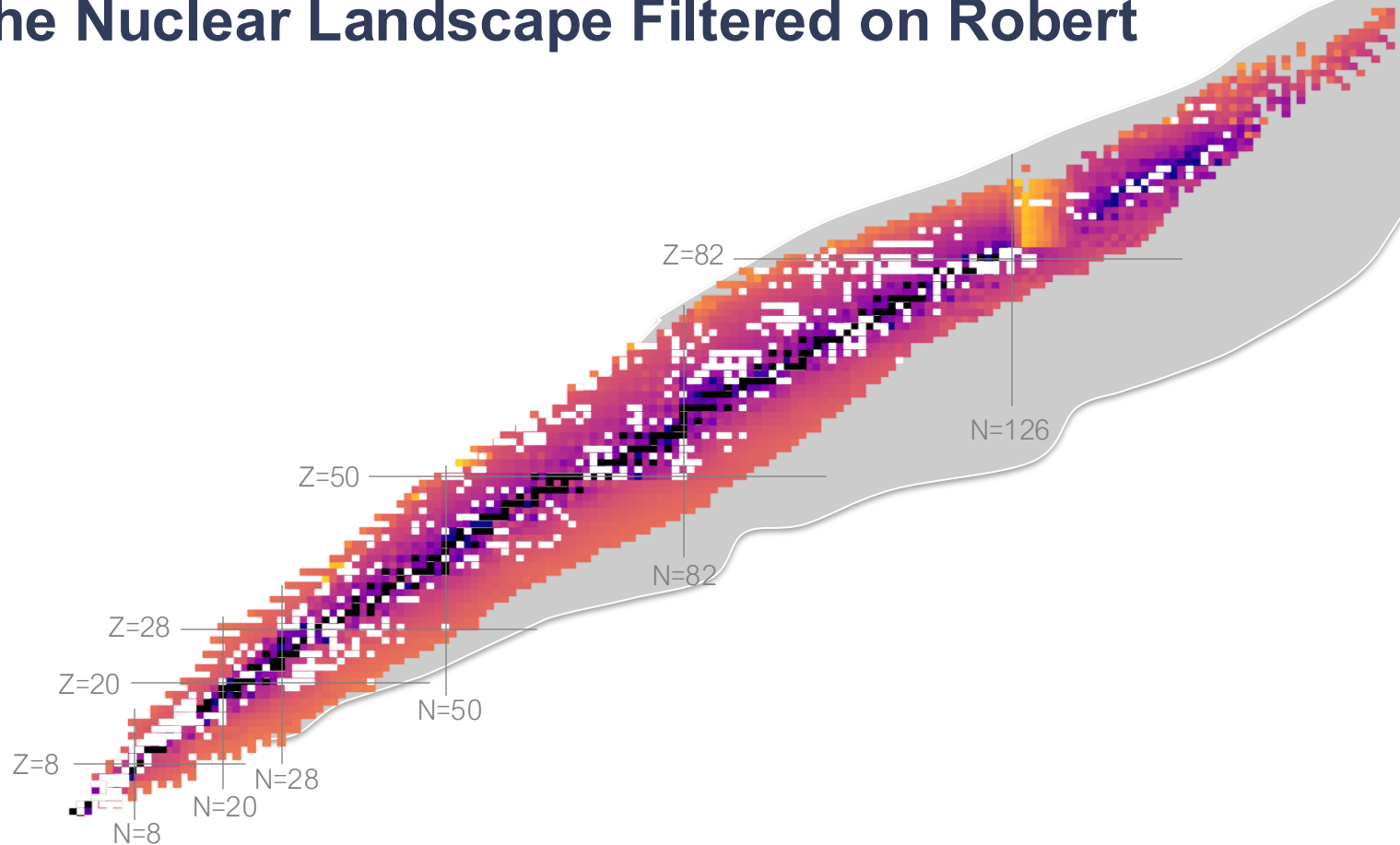
Heather Crawford  
Nuclear Science Division, Lawrence Berkeley National Laboratory

Nuclear Physics Over the Years: From the high spin era to rare isotopes  
September 20, 2025

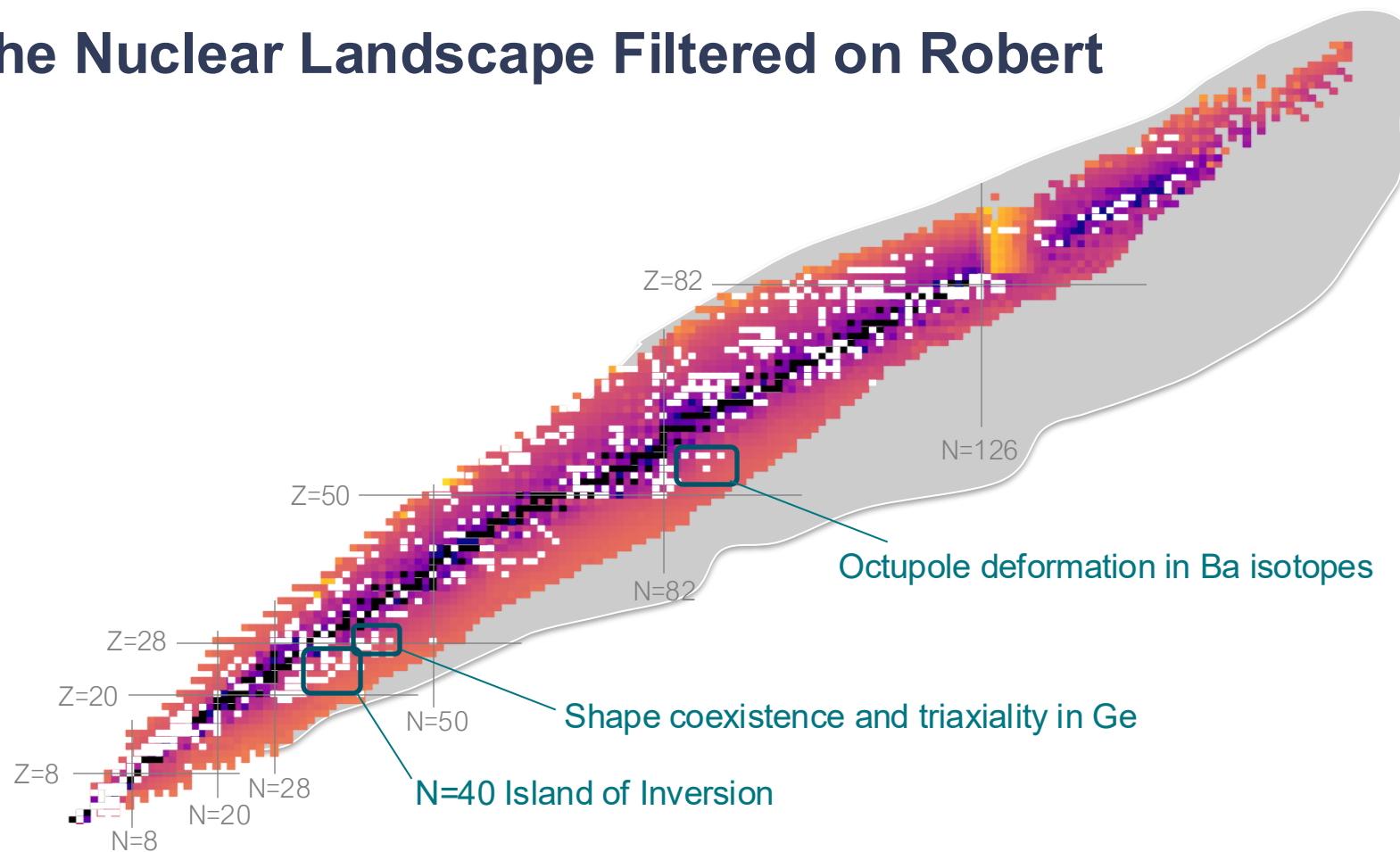
# The Nuclear Landscape



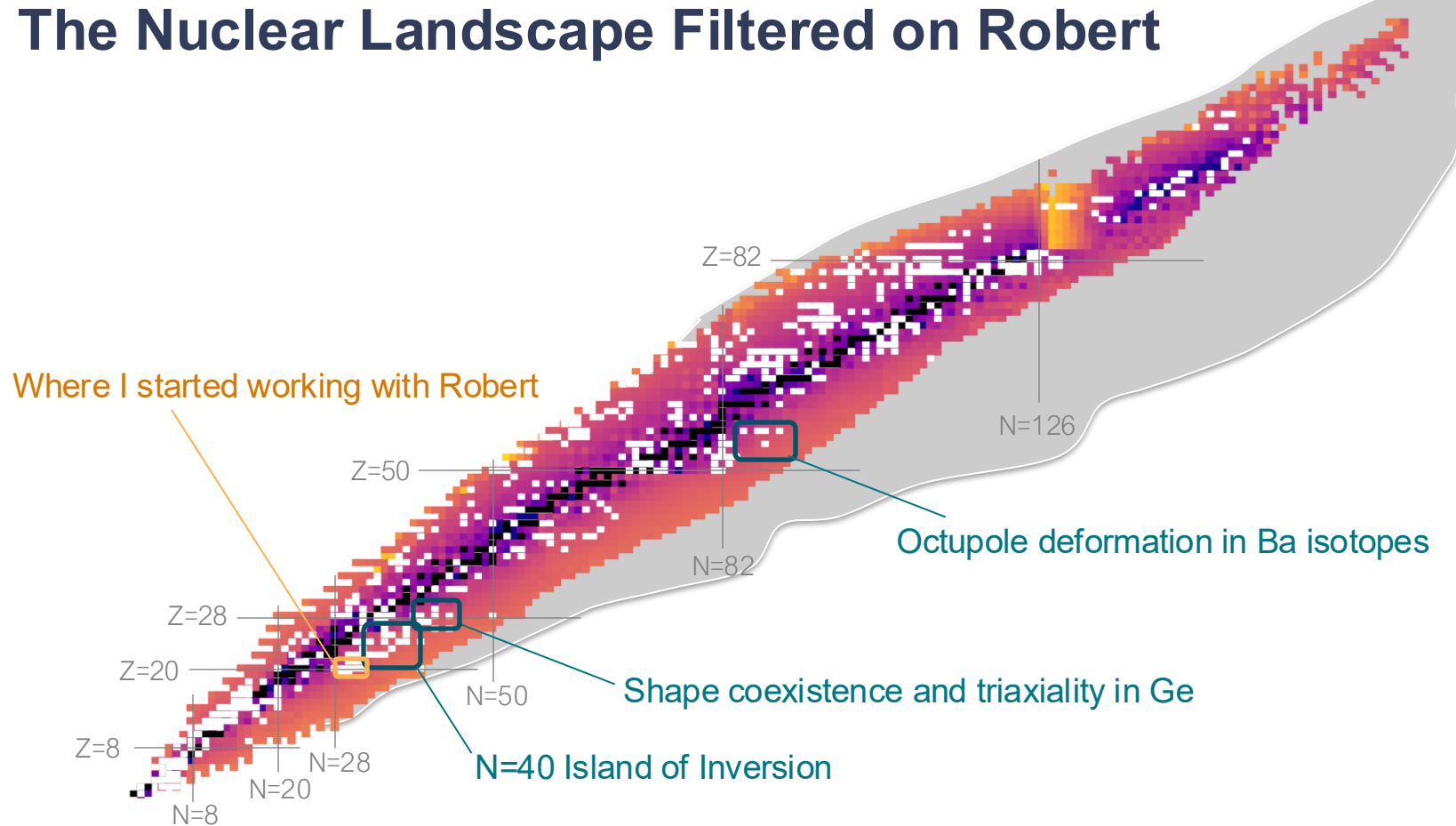
# The Nuclear Landscape Filtered on Robert



# The Nuclear Landscape Filtered on Robert



# The Nuclear Landscape Filtered on Robert



# Decay Properties of Neutron-Rich Sc and Ca Isotopes

PHYSICAL REVIEW C **82**, 014311 (2010)

## $\beta$ decay and isomeric properties of neutron-rich Ca and Sc isotopes

H. L. Crawford,<sup>1,2</sup> R. V. F. Janssens,<sup>3</sup> P. F. Mantica,<sup>1,2</sup> J. S. Berryman,<sup>1,2</sup> R. Broda,<sup>4</sup> M. P. Carpenter,<sup>3</sup> N. Cieplicka,<sup>4</sup> B. Fornal,<sup>4</sup> G. F. Grinyer,<sup>2</sup> N. Hoteling,<sup>3,5</sup> B. P. Kay,<sup>3</sup> T. Lauritsen,<sup>3</sup> K. Minamisono,<sup>2</sup> I. Stefanescu,<sup>3,5</sup> J. B. Stoker,<sup>1,2</sup> W. B. Walters,<sup>5</sup> and S. Zhu<sup>3</sup>

<sup>1</sup>*Department of Chemistry, Michigan State University, East Lansing, Michigan 48824, USA*

<sup>2</sup>*National Superconducting Cyclotron Laboratory, Michigan State University, East Lansing, Michigan 48824, USA*

<sup>3</sup>*Physics Division, Argonne National Laboratory Argonne, Illinois 60439, USA*

<sup>4</sup>*Institute of Nuclear Physics, Polish Academy of Sciences Cracow, Poland PL-31342*

<sup>5</sup>*Department of Chemistry and Biochemistry, University of Maryland, College Park, Maryland 20742, USA*

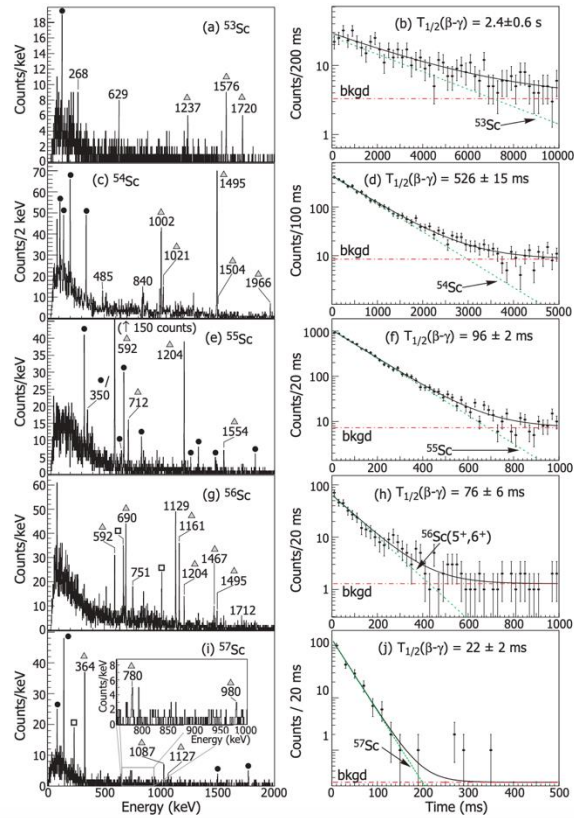
(Received 14 November 2009; revised manuscript received 10 May 2010; published 21 July 2010)

The isomeric and  $\beta$ -decay properties of neutron-rich  $^{53-57}\text{Sc}$  and  $^{53,54}\text{Ca}$  nuclei near neutron number  $N = 32$  are reported, and the low-energy level schemes of  $^{53,54,56}\text{Sc}$  and  $^{53-57}\text{Ti}$  are presented. The low-energy level structures of the  $_{21}\text{Sc}$  isotopes are discussed in terms of the coupling of the valence  $1f_{7/2}$  proton to states in the corresponding  $_{20}\text{Ca}$  cores. Implications with respect to the robustness of the  $N = 32$  subshell closure are discussed, as well as the repercussions for a possible  $N = 34$  subshell closure.

DOI: [10.1103/PhysRevC.82.014311](https://doi.org/10.1103/PhysRevC.82.014311)

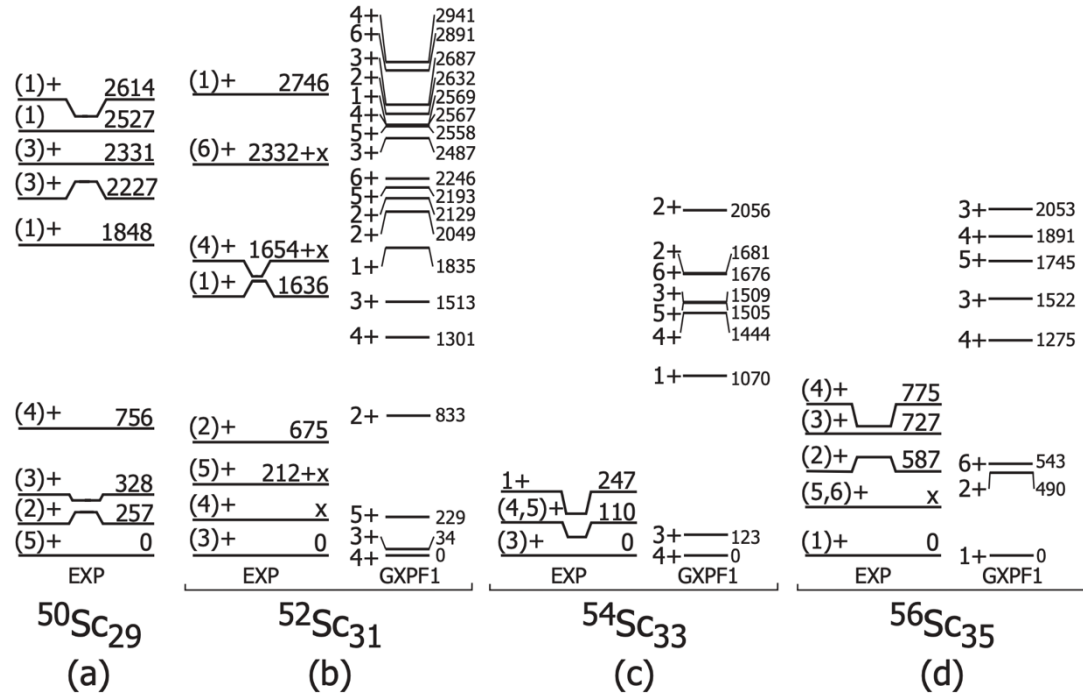
PACS number(s): 23.40.-s, 23.20.Lv, 27.40.+z, 29.38.Db

# Decay Properties of Neutron-Rich Sc and Ca Isotopes



- A measurement of the decay of neutron-rich Sc and Ca isotopes was discretionary time at NSCL to attempt to measure the decay of  $^{54}\text{K}$  into  $^{54}\text{Ca}$
- Unfortunately, this objective wasn't met, but there was more than enough for a PhD thesis !
- Systematic study of the decays into Sc and Ti allowed level schemes to be explored and discussion of the potential (at that time)  $N=32,34$  'magic' numbers

# Decay Properties of Neutron-Rich Sc and Ca Isotopes



- Consider structure in terms of coupling of  $f_{7/2}$  proton to  $pf(g)$ -shell neutrons
- 1+ states can only arise from coupling with  $f_{5/2}$  neutron – points to relatively close spacing with  $p_{1/2}$  and weak  $N=34$  gap in Sc – compressed spectrum in  $^{54,56}\text{Sc}$  compared to GXPF1 which included  $> 1\text{MeV}$  gap

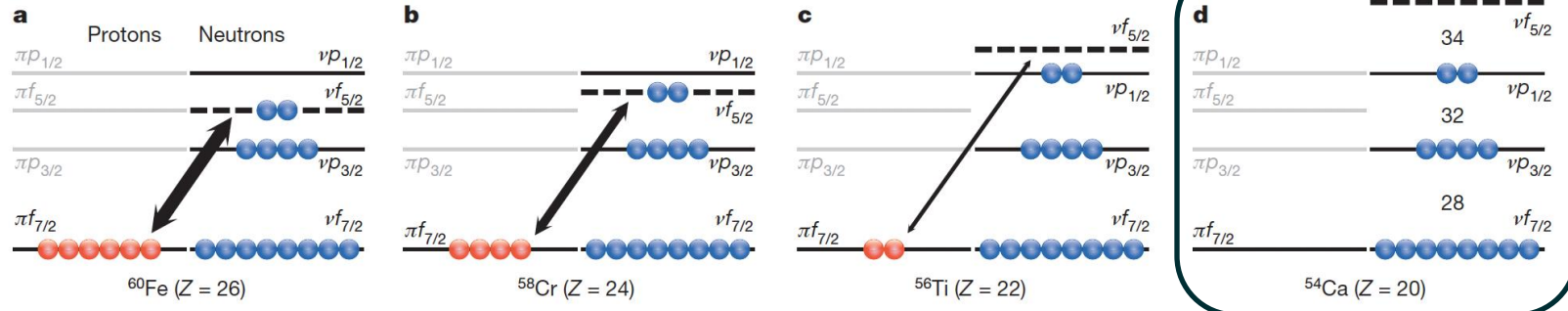
# The N=34 Shell Closure?

LETTER

doi:10.1038/nature12522

## Evidence for a new nuclear ‘magic number’ from the level structure of $^{54}\text{Ca}$

D. Steppenbeck<sup>1</sup>, S. Takeuchi<sup>2</sup>, N. Aoi<sup>3</sup>, P. Doornenbal<sup>2</sup>, M. Matsushita<sup>1</sup>, H. Wang<sup>2</sup>, H. Baba<sup>2</sup>, N. Fukuda<sup>2</sup>, S. Go<sup>1</sup>, M. Honma<sup>4</sup>, J. Lee<sup>2</sup>, K. Matsui<sup>5</sup>, S. Michimasa<sup>1</sup>, T. Motobayashi<sup>2</sup>, D. Nishimura<sup>6</sup>, T. Otsuka<sup>1,5</sup>, H. Sakurai<sup>2,5</sup>, Y. Shiga<sup>7</sup>, P.-A. Söderström<sup>2</sup>, T. Sumikama<sup>8</sup>, H. Suzuki<sup>2</sup>, R. Taniuchi<sup>5</sup>, Y. Utsuno<sup>9</sup>, J. J. Valiente-Dobon<sup>10</sup> & K. Yoneda<sup>2</sup>



# The N=34 Shell Closure?

LETTER

doi:10.1038/nature12522

Ev  
lev

D. Ste  
J. Lee  
T. Sur

PHYSICAL REVIEW C **96**, 064310 (2017)

## Structure of $^{55}\text{Sc}$ and development of the $N = 34$ subshell closure

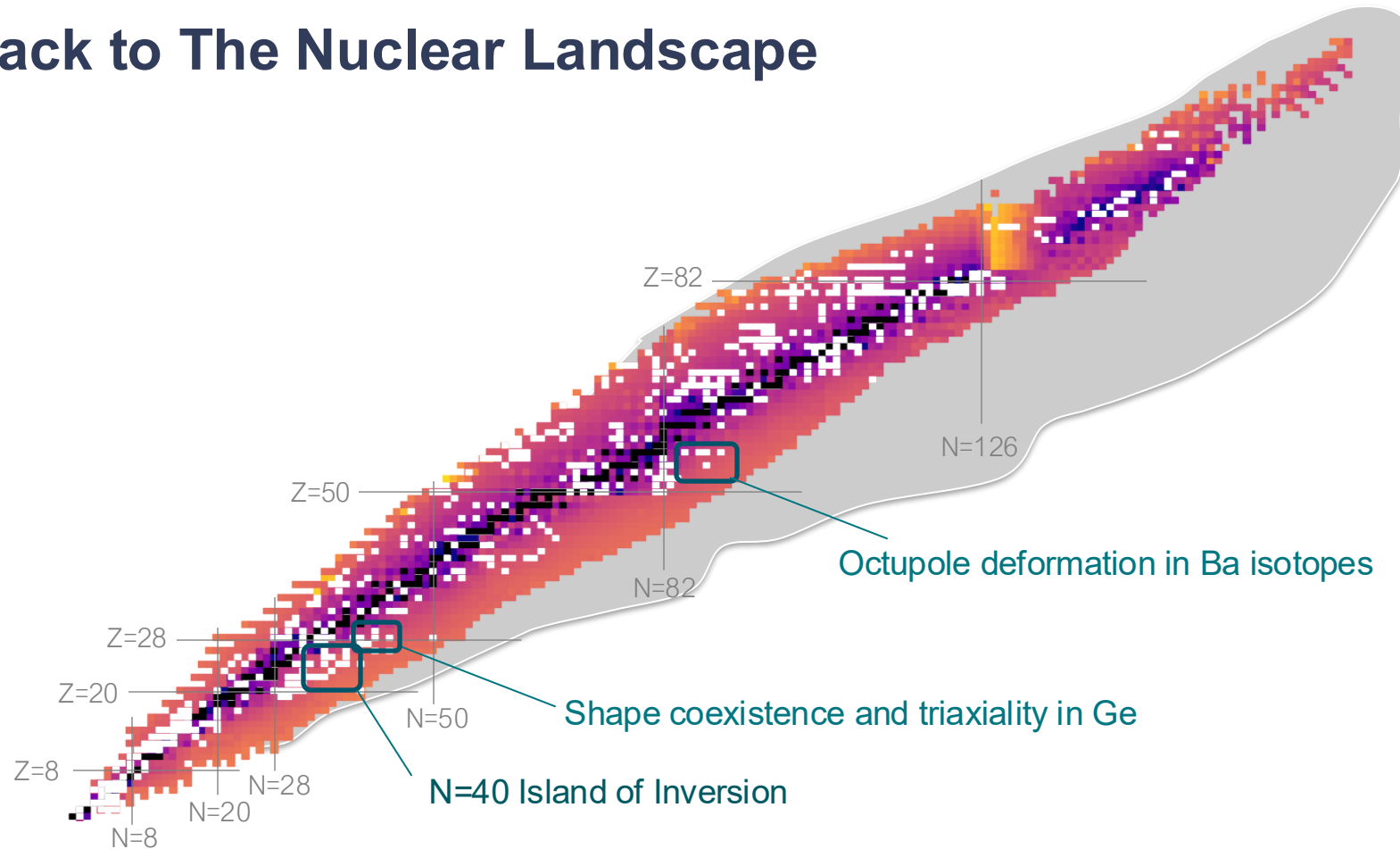
D. Steffenbeck,<sup>1,\*</sup> S. Takeuchi,<sup>2</sup> N. Aoi,<sup>3</sup> P. Doornenbal,<sup>1</sup> M. Matsushita,<sup>4</sup> H. Wang,<sup>1</sup> H. Baba,<sup>1</sup> S. Go,<sup>4,†</sup> J. D. Holt,<sup>5</sup> J. Lee,<sup>1,‡</sup> K. Matsui,<sup>6</sup> S. Michimasa,<sup>4</sup> T. Motobayashi,<sup>1</sup> D. Nishimura,<sup>7</sup> T. Otsuka,<sup>4,6,†</sup> H. Sakurai,<sup>1,6</sup> Y. Shiga,<sup>8</sup> P.-A. Söderström,<sup>1,§</sup> S. R. Stroberg,<sup>5</sup> T. Sumikama,<sup>9,†</sup> R. Taniuchi,<sup>1,6</sup> J. A. Tostevin,<sup>10</sup> Y. Utsuno,<sup>11</sup> J. J. Valiente-Dobón,<sup>12</sup> and K. Yoneda<sup>1</sup>



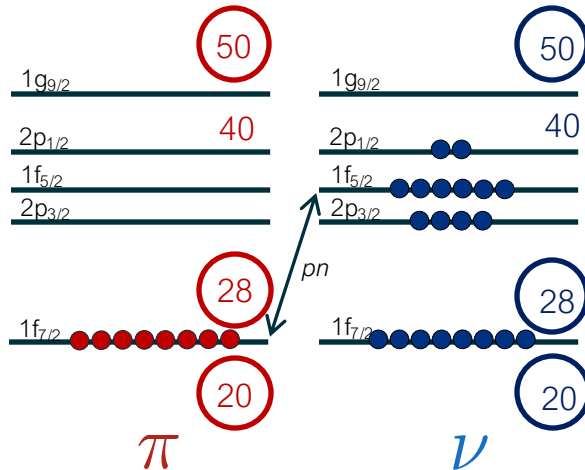
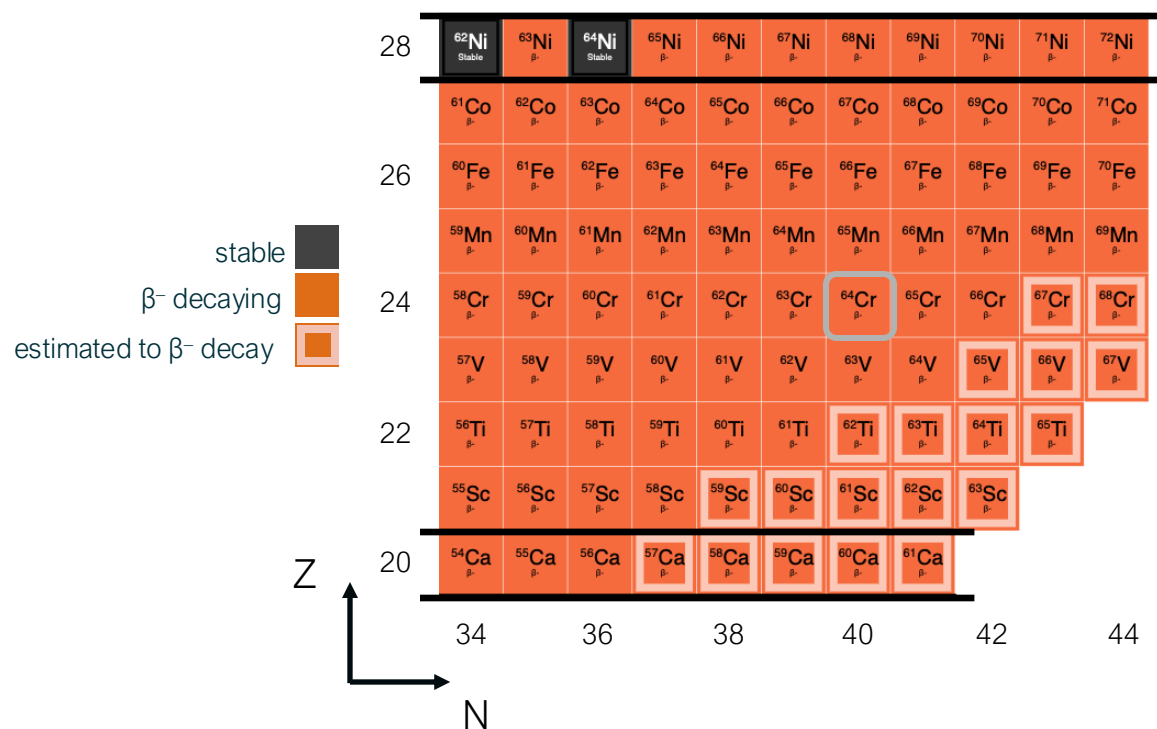
The results indicates a rapid weakening of the  $N=34$  subshell closure in  $pf$ -shell nuclei at  $Z > 20$ , even when only a single proton occupies the  $\pi f_{7/2}$  orbital.



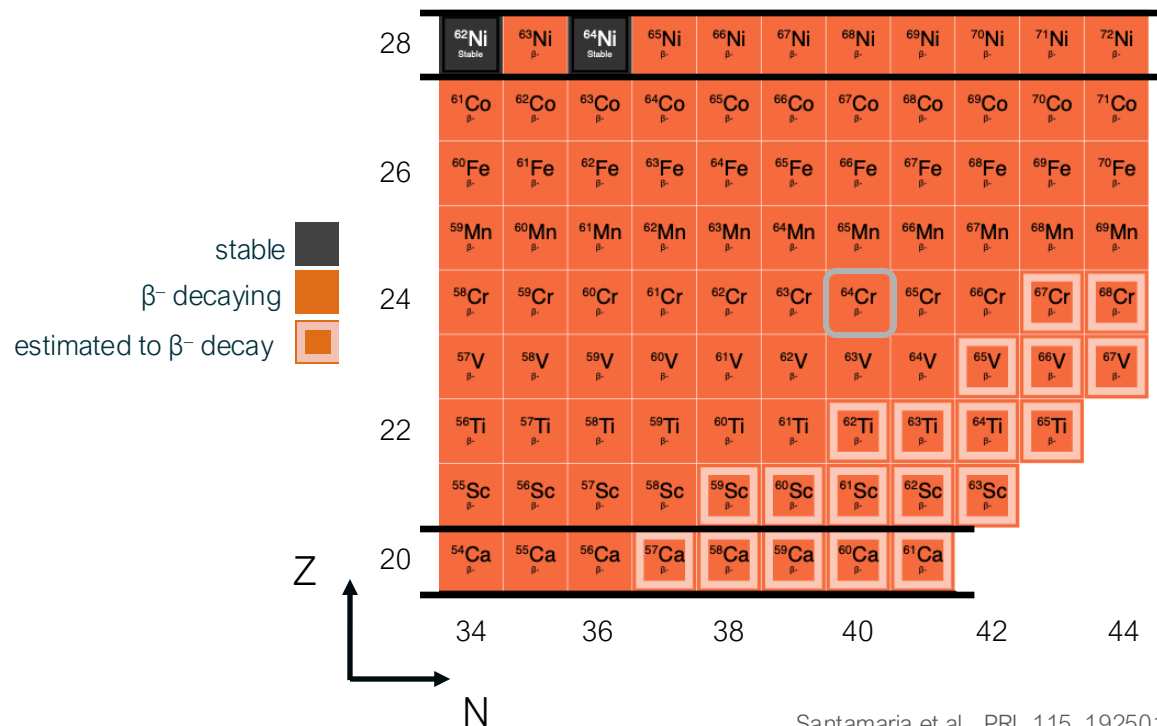
# Back to The Nuclear Landscape



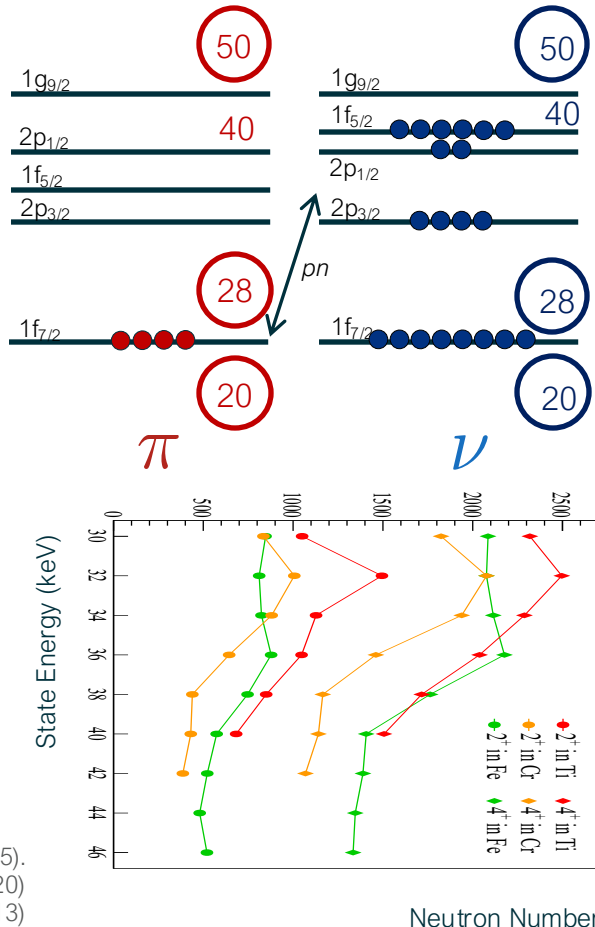
# The N=40 Island of Inversion



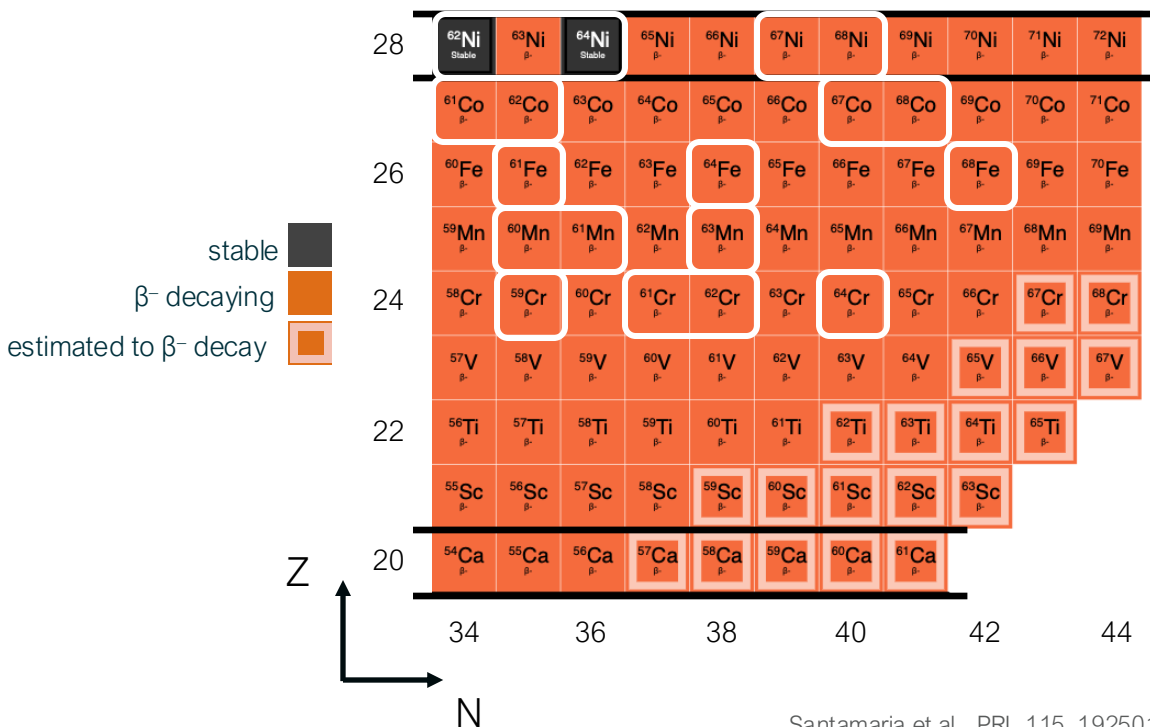
# The N=40 Island of Inversion



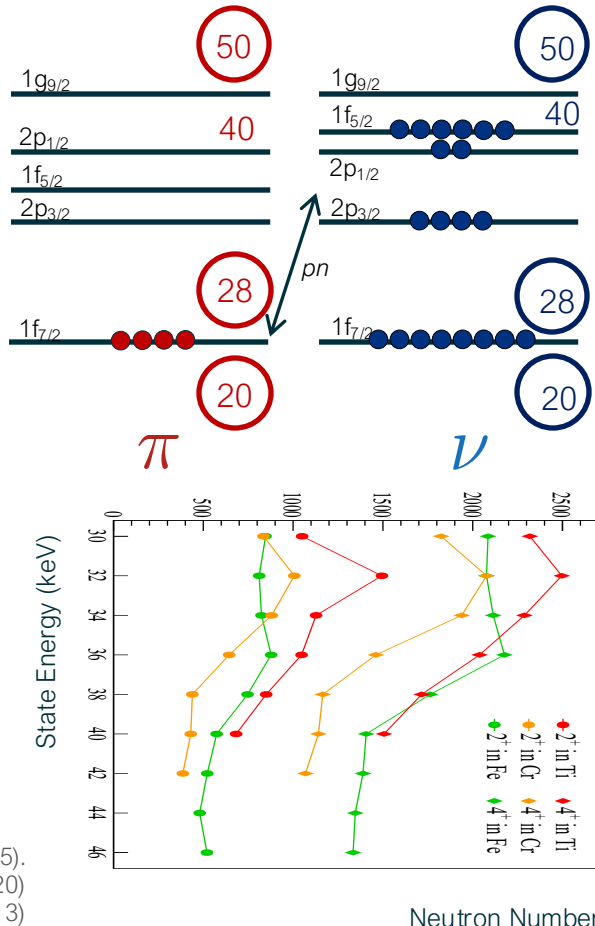
Santamaria et al., PRL 115, 192501 (2015).  
 Cortés et al., PLB 800, 135071 (2020)  
 Crawford et al., PRL 110, 242701 (2013)



# The N=40 Island of Inversion

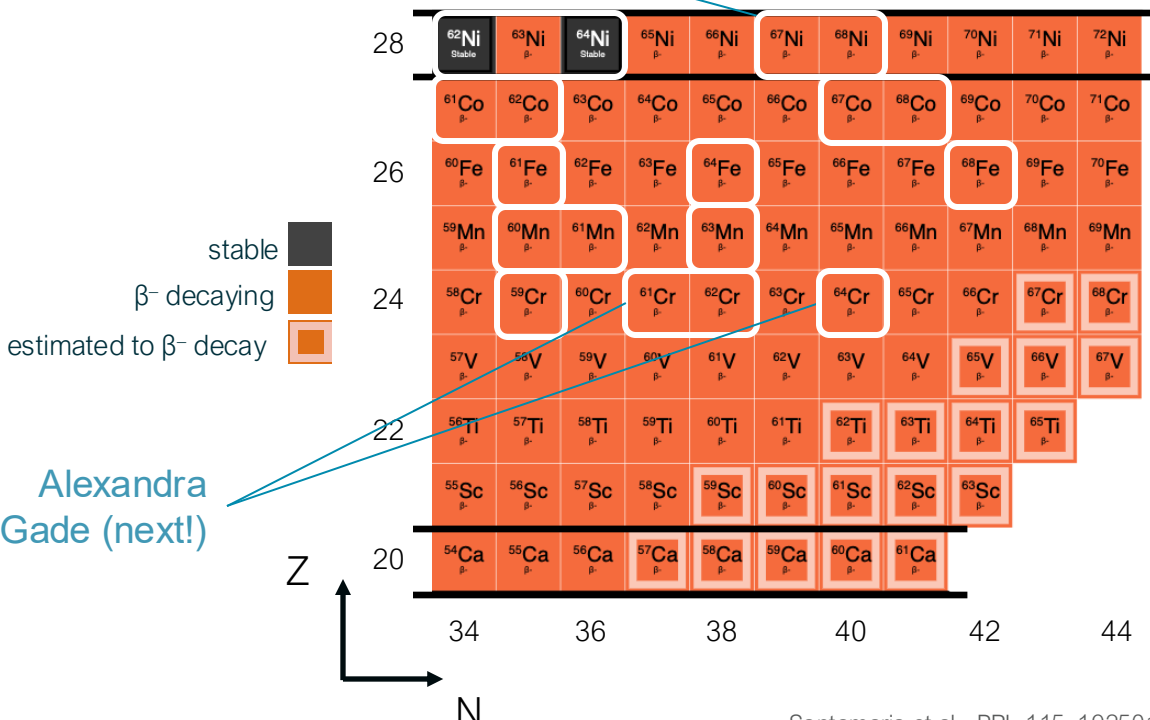


Santamaria et al., PRL 115, 192501 (2015).  
 Cortés et al., PLB 800, 135071 (2020)  
 Crawford et al., PRL 110, 242701 (2013)

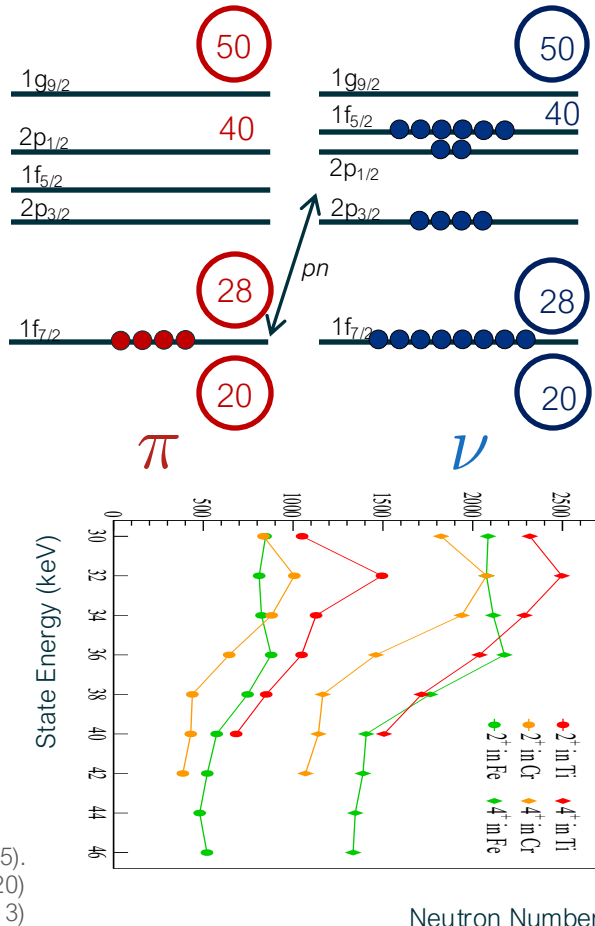


# The N=40 Island of Inversion

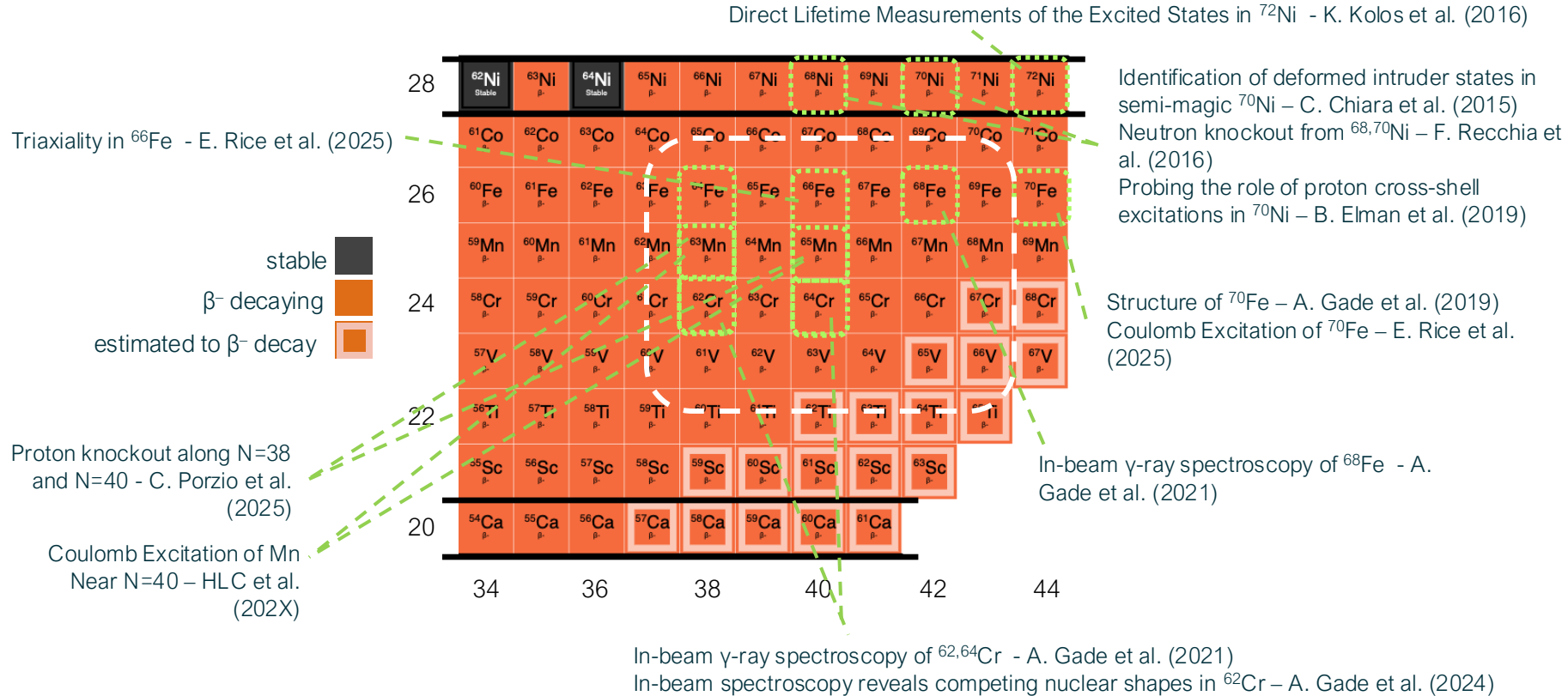
Ben Crider (yesterday)



Santamaria et al., PRL 115, 192501 (2015).  
 Cortés et al., PLB 800, 135071 (2020)  
 Crawford et al., PRL 110, 242701 (2013)

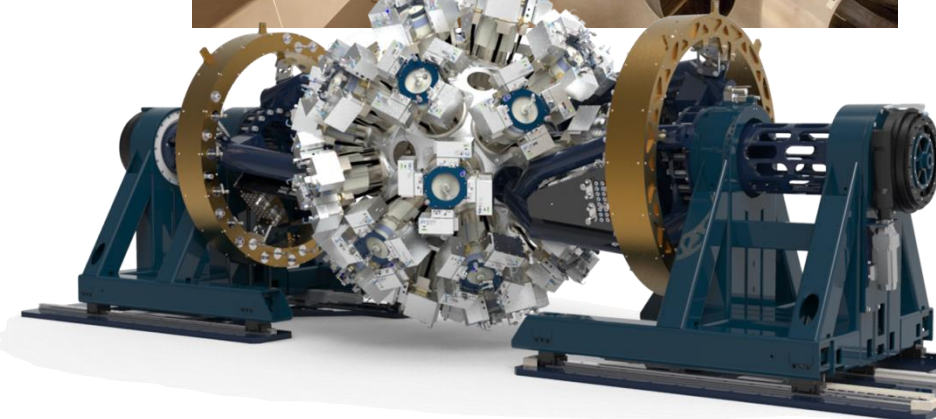


# The N=40 Island of Inversion with GRETINA



# GRETINA and GRETA

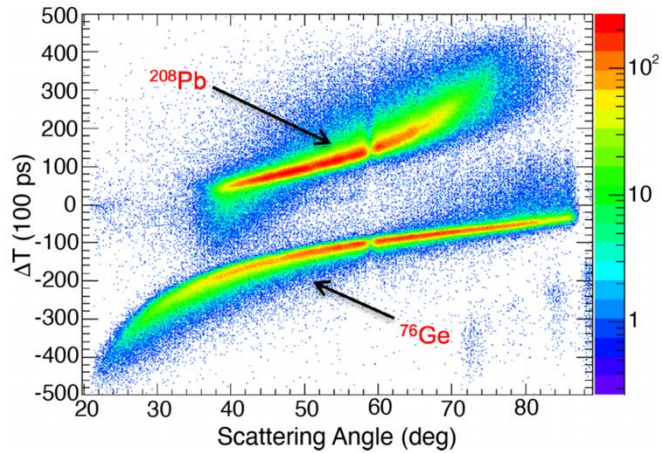
- The physics impact of GRETINA over the past > 10 years has been substantial
- GRETINA was constructed 2003-2011, with a subsequent “enhancement” phase
- GRETA, the full  $4\pi$  realization of a tracking array received CD-4A in August and will start source commissioning at FRIB in the next few months
- Robert has been a **vocal supporter and advocate for GRETA** since the beginning



# Triaxiality in Ge

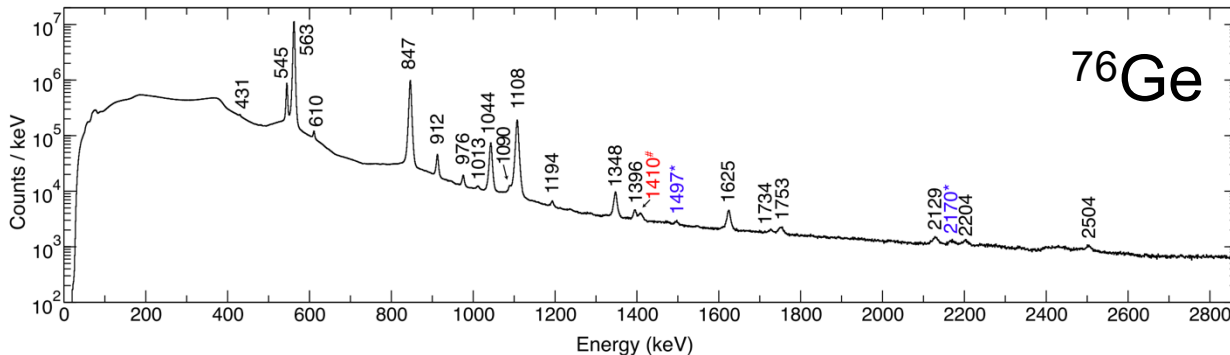
- Above the N=40壳层,  $^{76}\text{Ge}$  has been a focus across nuclear physics as a candidate for  $0\nu\beta\beta$  decay, which highlighted the need to understand the structure in this (and neighbouring nuclei) to reliably calculate the necessary nuclear matrix elements
- The Ge isotopes in this region were known to have complex wavefunctions and variation in their excitation spectra; theory predictions also suggested the importance of triaxiality
- GRETINA + CHICO2 at ATLAS offered a path forward to characterize, in detail these systems using Coulomb excitation

# Triaxiality in Ge



- Coulomb excitation of  $^{76}\text{Ge}$ , detailed GOSIA analysis and comparison to theory/model predictions confirmed a rigid triaxial deformation
- This contrasts with the soft triaxial potential in  $^{76}\text{Se}$  which will impact NME important to  $0\nu\beta\beta$

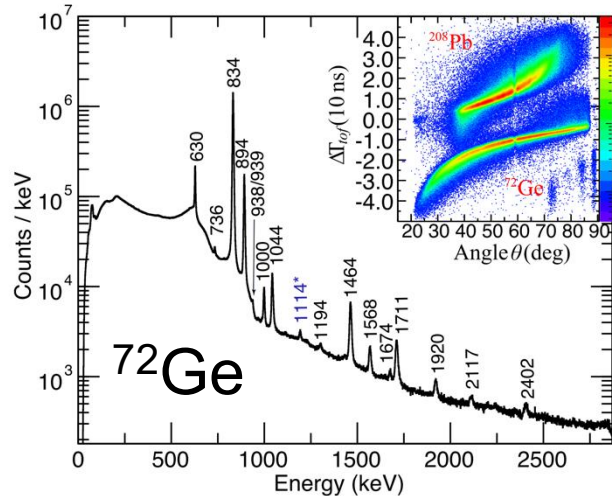
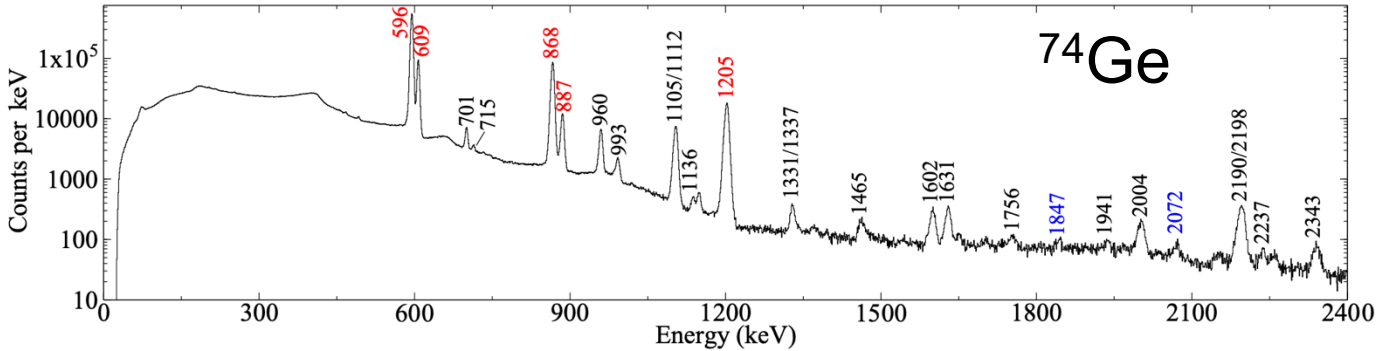
A. D. Ayangeakaa, R. V. F. Janssens *et al.*, Phys. Rev. Lett. **123**, 102501 (2019).  
J. Henderson *et al.*, Phys. Rev. C **99**, 054313 (2019).  
A. D. Ayangeakaa, R. V. F. Janssens *et al.*, Phys. Rev. C **107**, 044314 (2023).



# Triaxiality in Ge

- Experiments in neighbouring  $^{72,74}\text{Ge}$  further confirmed the importance of triaxiality, suggesting triaxial shape coexistence between the two lowest  $0^+$  states in both systems

A. D. Ayangeakaa, R. V. F. Janssens *et al.*, Phys. Lett. B **754**, 254 (2016).  
N. Sensharma *et al.*, Phys. Rev. C **112**, 024311 (2025).

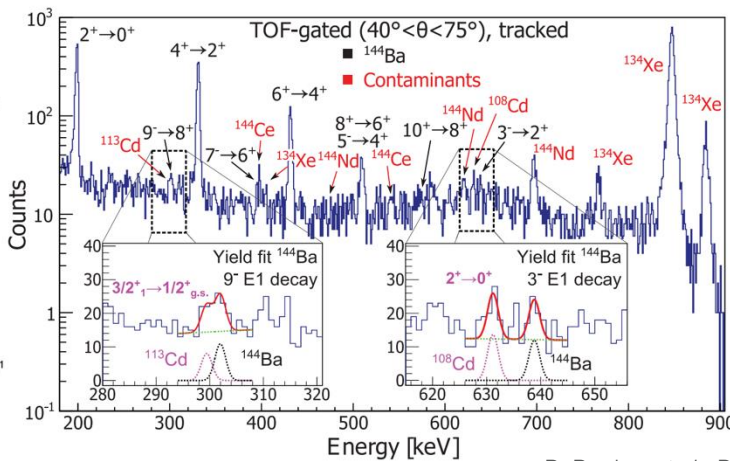
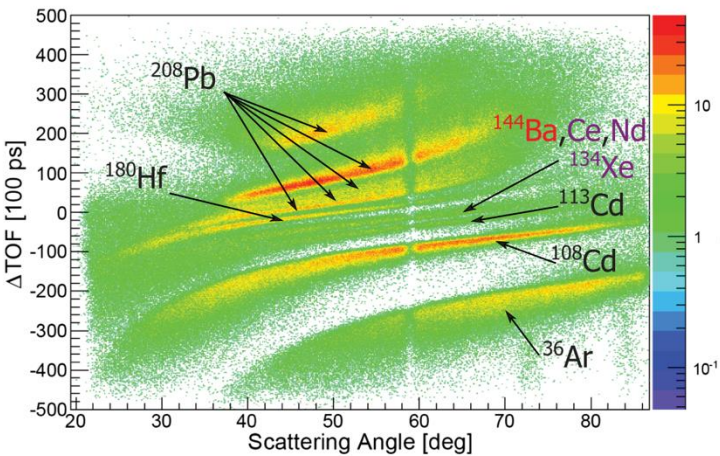


# Octupoles in Ba

- The neutron-rich Ba isotopes are one region of the chart where octupole correlations were expected, with 56 protons and 88 neutrons in  $^{144}\text{Ba}$ , two ‘octupole magic numbers’ where single-particle states separated by  $\Delta l = \Delta j = 3$  orbitals are near the Fermi surface
- Before 2016, only indirect evidence for octupole correlations in the Ba isotopes had been observed (e.g. enhanced E1 transitions between g.s. and negative-parity band)
- Enter CARIBU + GRETINA + CHICO2...

# Octupoles in Ba

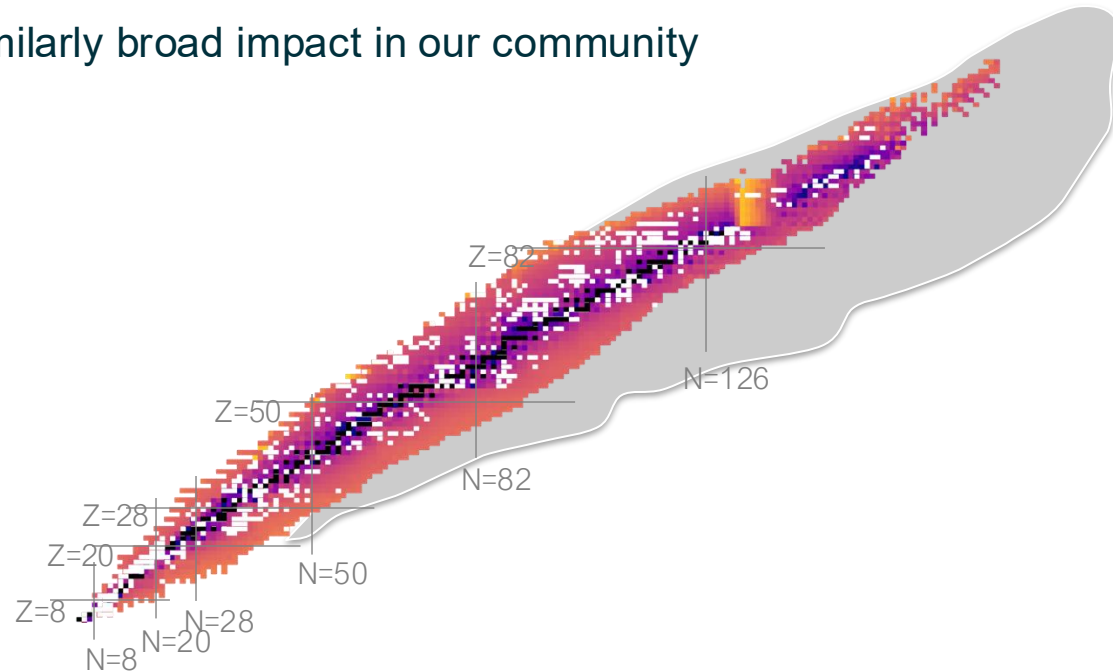
- Coulomb excitation of  $^{144}\text{Ba}$ , and the yield of the gamma rays depopulating the  $3^-$  and related states enabled extraction of a E3 matrix element
- The value of  $B(\text{E3}:3^- \rightarrow 0^+) = 48^{+25}_{-34}$  W.u. was much higher than model predictions, motivating further measurements in neighbouring isotopes (e.g.  $^{143}\text{Ba}$ ), and additional measurements in  $^{144}\text{Ba}$



B. Bucher *et al.*, Phys. Rev. Lett. **116**, 112503 (2016).  
C. Morse *et al.*, Phys. Rev. C **102**, 054328 (2020).

# Summary

- The range of collectivity and deformation across the nuclear chart is broad, with variation in both the origin and nature of the emergent structures
- Robert has had a similarly broad impact in our community



# Summary

- The range of collectivity and deformation across the nuclear chart is broad, with variation in both the origin and nature of the emergent structures
- Robert has had a similarly broad impact in our community... and at the same time never lost sight of the details

based calculations. While both give reasonable agreement with data in terms of excitation spectra, there is a difference in the predictions of the detailed distribution of strength in the  $\nu f_{1/2}$  strength. The difference between GXPF1 and large-scale shell-model calculations using microscopically-derived NN+3N shell-model interactions [1, 2]. Phenomenological models are consistent with the single-particle description, where one would expect the full  $\nu f_{1/2}$  strength to be concentrated in the  $^{40}\text{Ca}$  ground state.  $^{40}\text{Ca}$  nuclei at and immediately beyond  $N=28$ . The micro- and macroscopic models suggest a fragmentation of the  $\nu f_{1/2}$  strength to higher-lying states in these nuclei.

We report in this letter on the results of a neutron knockout ( $\text{C}(\text{n},\text{p})$ ) experiment performed along the  $^{40}\text{Ca}$  chain from  $N=28$  to  $N=30$  using the high-intensity  $\gamma$ -ray source GREITINA to measure exclusive neutron knockout cross sections from  $^{40}\text{Ca}$  to states in  $^{40}\text{Ca}$ , and from  $^{40}\text{Ca}$  to  $^{47}\text{Ca}$ . Based on the experimental cross-section data and theoretical calculations, calculated under the assumption of the sudden removal of a neutron from a given set of quantum numbers, we can extract spectroscopic factors, which for neutron-capture reactions should correspond directly to the occupancy of a given neutron single-particle orbital. A relative measurement, such as that performed here comparing  $^{40}\text{Ca}(\text{n},\text{p})$  to  $^{40}\text{Ca}(\text{n},\text{p})$  neutron removal processes, transfers us from the details of the trend in the spectroscopic strength distributions for the trend in the spectroscopic strength distributions for the trend in the  $f_0$  orbitals. Our results indicate a decrease in the population of the lowest  $(\nu f_{1/2})^2$  state in  $^{40}\text{Ca}$ , supporting the description of NN+3N calculations in the  $f$  shell model space. We compare our results with both phenomenological descriptions and microscopic interactions in a larger model space including the  $1p_{1/2}$  orbital.

Neutron-knockout was performed at the National Superconducting Cyclotron Laboratory (NSCL) at Michigan State University. Secondary beams of  $^{48,50}\text{Ca}$  were produced following fragmentation of  $^{208}\text{Po}$  at 160 MeV, and primarily based on a 423 mg/cm<sup>2</sup>  $^{208}\text{Po}$  target, and then separated from other species through the A1900 fragment separator [10], based on magnetic rigidity and relative energy loss through an Al degrader wedge.

Fractures were delivered to the experiment along with a monochromator, a set of  $\nu f_{1/2}$  and  $\nu p_{1/2}$  beam-pipe segments, and a beam position monitor (BPM) at the target position of the S803 spectrograph [11]. The resulting knockout products ~~continued~~ were identified on an event-by-event basis through the time-of-flight and energy loss as measured by the focal plane detectors.

Seven GREITINA [9] quad modules surrounded the target position of the S803 and were used to detect  $\gamma$  rays emitted from excited states populated in the knockout residues. Four modules were placed at forward ( $\theta \sim 58^\circ$ ) angles, and three at  $\theta = 90^\circ$  relative to the beam direction.

Each GREITINA module consists of four closely packed, high-purity germanium crystals (28 in total), with each crystal electrically segmented into 30 individual elements. The degree of segmentation is limited with the decomposition of the full set of signals allows the positions and energies of individual  $\gamma$ -ray interaction points to be measured and tracked. The  $\gamma$ -ray interaction position information from GREITINA, along with the particle trajectory information from the S803 were used to reconstruct the  $\gamma\gamma$  events. The Doppler reconstruction of the observed  $\gamma\gamma$  events. An overall  $\gamma$ -ray resolution of  $\sim 1.5\%$  was achieved following Doppler correction. Yields for individual transitions were determined based on a fit to data using a computer GEANT4 simulation. The energy calibration, resolution, and time loss into account the expected angular distribution of emitted  $\gamma$ -rays; the simulation reproduces source efficiencies to within  $\sim 1\%$ . The results are summarized in Fig. 1 and Table I.

The spectra of  $\gamma$ -rays detected in GREITINA in coincidence with  $^{40}\text{Ca}$  removal are shown in Fig. 2 in panels (a) and (b). The corresponding level schemes in  $^{40}\text{Ca}$  and  $^{47}\text{Ca}$ , as observed in this work, are shown in Fig. 3(c) and (d). Twelve transitions are observed and associated with levels in  $^{47}\text{Ca}$  populated in the one neutron removal reaction. The majority of the transitions were previously observed [12] and the placement in the level scheme follows the literature. Two levels at 3425 and 3207 keV were not previously reported, but are placed as transitions directly to the ground state based on their energy (population) and angular distribution via these transitions. The ground state in  $^{47}\text{Ca}$  is at 2.59 MeV, and the doublet levels in the original level list at 2.59 MeV (above the highest observed and confirmed state), and supported by  $\beta$ -decay data [13]. Where statistics are sufficient, the level schemes are  $\gamma$ - $\gamma$  correlated. For  $^{40}\text{Ca}(\text{n},\text{p})$ , the states of primary interest are at 2.59, 2.38, and 0 MeV, the ground state, and the doublet levels at 2.38 and 2.59 MeV, respectively. We note that the state at 2.0 MeV may also be populated through direct removal of a  $2p_{1/2}$  neutron, should such a configuration be present in the  $^{40}\text{Ca}$  ground state.

For the case of  $^{40}\text{Ca}$ , six transitions, all of which have been previously placed in the level scheme [14, 15]. Here, the states at 3.4 MeV state and the 2.38 MeV state of primary interest, and the doublet levels at 2.0 and 2.59 MeV, respectively. We note that the state at 2.0 MeV may also be populated through direct removal of a  $2p_{1/2}$  neutron, should such a configuration be present in the  $^{40}\text{Ca}$  ground state. Cross-sections for the direct population of the states of interest in  $^{47}\text{Ca}$  are given in Table I and were deduced from the observed level schemes, according to the formula of the single-particle theory. The relative parallel momentum distributions were found to be consistent with the expected angular momentum transfer for these states, i.e.,  $l = 0, 2$ , and 3 for the 2.59, 2.38 MeV, and ground state, respectively, in the  $^{40}\text{Ca}(\text{n},\text{p})$ .

I don't think this detail is needed in a  $\text{PR}$ !

My cleanest page of feedback from Robert – only 2 hyphen issues (personal best)!!

# Summary

- The range of collectivity and deformation across the nuclear chart is broad, with variation in both the origin and nature of the emergent structures
- Robert has had a similarly broad impact in our community... and at the same time never lost sight of the details

# Thank you!

based calculations. While both give reasonable agreement with data in terms of excitation spectra, there is a difference in the predictions of the detailed distribution of strength in the  $\nu f_{1/2}$  strength. The two GXPF1 and large-scale shell-model calculations using microscopically-derived NN+3N shell-model interactions [1, 2]. Phenomenological models are consistent with the single-particle description, where one would expect the full  $\nu f_{1/2}$  strength to be concentrated in the  $0^+$  state. The micro- and macro- shell models both suggest a fragmentation of the  $\nu f_{1/2}$  strength to higher-lying states in these nuclei.

We report in this letter on the results of a neutron knockout ( $\text{Ca-1n}$ ) experiment performed along the  $^{40}\text{Ca}$  chain from  $N=28$  to  $N=30$  using the high-intensity  $\gamma$ -ray source GREITINA to measure excitation neutron knockout cross-sections from  $^{40}\text{Ca}$  to states in  $^{40}\text{Ca}$ , and from  $^{40}\text{Ca}$  to  $^{42}\text{Ca}$ . Based on the experimental cross-section data and theoretical cross-sections, calculated under the assumption of the sudden removal of a neutron from a given set of quantum numbers, we can extract spectroscopic factors, which for neutron-capture reactions should correspond directly to the occupancy of a given neutron single-particle orbital. A relative measurement, such as that performed here comparing  $^{40}\text{Ca-}(1n)$  to  $^{40}\text{Ca-}(1n)$  neutron removal processes, translates to firmly establishing the trend in the spectroscopic strength distributions for the trend in the spectroscopic strength distributions for the trend in the  $f_0$  orbitals. Our results indicate a decrease in the population of the lowest  $(\nu f_{1/2})^2$  state in  $^{40}\text{Ca}$ , supporting the description of NN+3N corrections in the  $f_0$  shell model space. This is consistent with both phenomenological descriptions and microscopic interactions in a larger model space including the  $1p_{1/2}$  orbital.

Neutron-knockout was performed at the National Superconducting Cyclotron Laboratory (NSCL) at Michigan State University. Secondary beams of  $^{44,46,48}\text{Ca}$  were produced following fragmentation of  $^{208}\text{Po}$  at 160 MeV, and primarily based on a 423 mg/cm<sup>2</sup>  $^{90}\text{Zr}$  target and then separated from other species through the A1900 fragment separator [10], based on magnetic rigidity and relative energy loss through an Al degrader wedge. Fragments were delivered to the experimental area with a momentum spread of  $\pm 2\%$ ,  $\Delta p/p$ , and an  $\approx 3^\circ$  solid angle. Beam was focused to  $\approx 10\text{ cm}$  at the target position of the S800 spectrograph [11]. The resulting knockout products ~~continued~~ were identified on an event-by-event basis through time-of-flight and energy loss as measured by the focal plane detectors.

Seven GREITINA [9] quad modules surrounded the target position of the S800 and were used to detect  $\gamma$  rays emitted from excited states populated in the knockout residues. Four modules were placed at forward ( $\theta \sim 58^\circ$ ) angles, and three at  $\theta = 90^\circ$  relative to the beam direction. Each GREITINA module consists of four closely packed, high-purity germanium crystals (28 in total), with each crystal electrically segmented into 30 individual elements. The degree of segmentation is limited with the decomposition of the full set of signals allows the positions and energies of individual  $\gamma$ -ray interaction points to be measured and tracked. The  $\gamma$ -ray interaction position information from GREITINA, along with the particle trajectory information from the S800 were used to reconstruct the  $\gamma\gamma$  correlation function. Doppler reconstruction of the observed  $\gamma\gamma$  was an overall  $\gamma$ -ray resolution of  $\sim 1.5\%$  was achieved following Doppler correction. Yields for individual transitions were determined based on a fit to data using a commercial GEANT4 simulation. The energy resolution was  $\sim 10\%$ , and this was taken into account in the expected angular distribution of emitted  $\gamma$ -rays; the simulation reproduces source efficiencies to within  $\sim 1\%$ . The results are summarized in Fig. 1 and Table I.

The spectra of  $\gamma$ -rays detected in GREITINA in coincidence with  $^{40}\text{Ca}$  removal are shown in Fig. 2. The corresponding level schemes in  $^{40}\text{Ca}$  and  $^{42}\text{Ca}$  are shown in Fig. 3(c) and (d). Two-body transitions are observed and associated with levels in  $^{40}\text{Ca}$  populated in the one neutron removal reaction. The majority of the transitions were well reproduced [12] and the placement in the level scheme follows the literature. Two  $\gamma\gamma$  peaks at 3425 keV and 3207 keV were not previously reported, but are placed as transitions directly to the ground state based on their energy (population of a ground state via these transitions) and the small energy difference (less than 200 keV above the highest observed and confirmed state), and supported by  $\beta$ -decay data [13]. Where statistics are sufficient, the level schemes are  $\gamma\gamma$  correlated.

For  $^{40}\text{Ca-}(1n)$ , the states of primary interest are at 2.59 MeV, 2.38 MeV and 0 MeV (ground state), corresponding to removal of a  $2p_{3/2}$ ,  $1d_{5/2}$  and  $1f_{7/2}$  neutron, respectively.

For the case of  $^{40}\text{Ca-}(2n)$ , eight transitions, all of which have been previously placed in the level scheme [14, 15]. Here, the states at 3.4 MeV and state at 2.9 MeV are of primary interest, corresponding to removal of a  $2p_{1/2}$  and  $2p_{3/2}$  neutron, respectively.

We note that the state at 2.0 MeV may also be populated through direct removal of a  $2p_{1/2}$  neutron, should such a configuration be present in the  $^{40}\text{Ca}$  ground state.

Cross-sections for the direct population of the states of interest in  $^{42}\text{Ca}$  are given in Table I and were deduced from the corresponding level schemes. According to the literature [16] of excited states in  $^{42}\text{Ca}$ , the parallel momentum distributions were found to be consistent with the expected angular momentum transfer for these states, i.e.,  $l = 0, 2$ , and 3 for the 2.59, 2.38 MeV, and ground state, respectively, in the  $^{40}\text{Ca-}(1n)$ .

I don't think this detail is needed in a  $\text{PR}$ !

My cleanest page of feedback from Robert – only 2 hyphen issues (personal best)!!

# Thank you